Theoretical rotation-torsion energies of HSOH

Roman I. Ovsyannikov,[1,a)] Vladlen V. Melnikov,[1,b)] Walter Thiel,[2] Per Jensen,[1,c)] Oliver Baum,[3] Thomas F. Giesen,[3] and Sergei N. Yurchenko[4]
[1]*FB C–Theoretische Chemie, Bergische Universität, D-42097 Wuppertal, Germany*
[2]*Max-Planck-Institut für Kohlenforschung, Kaiser-Wilhelm-Platz 1, D-45470 Mülheim an der Ruhr, Germany*
[3]*I. Physikalisches Institut, Universität zu Köln, Zülpicher Strasse 77, D-50937 Köln, Germany*
[4]*Institut für Physikalische Chemie und Elektrochemie, Technische Universität Dresden, D-01062 Dresden, Germany*

(Received 25 July 2008; accepted 10 September 2008; published online 20 October 2008)

The rotation-torsion energies in the electronic ground state of HSOH are obtained in variational calculations based on a newly computed *ab initio* CCSD(T)/aug-cc-pV(Q+*d*)Z potential energy surface. Using the concept of the reaction path Hamiltonian, as implemented in the program TROVE (theoretical rovibrational energies), the rotation-vibration Hamiltonian is expanded around geometries on the torsional minimum energy path of HSOH. The calculated values of the torsional splittings are in excellent agreement with experiment; the root-mean-square (rms) deviation is 0.0002 cm^{-1} for all experimentally derived splittings (with $J \leq 40$ and $K_a \leq 4$). The model provides reliable predictions for splittings not yet observed. The available experimentally derived torsion-rotation term values (with $J \leq 40$ and $K_a \leq 4$) are reproduced *ab initio* with an rms deviation of 1.2 cm^{-1} (0.7 cm^{-1} for $J \leq 20$), which is improved to 1.0 cm^{-1} (0.07 cm^{-1} for $J \leq 20$) in an empirical adjustment of the bond lengths at the planar *trans* configuration. The theoretical torsional splittings of HSOH are analyzed in terms of an existing semiempirical model for the rotation-torsion motion. The analysis explains the irregular variation of the torsional splittings with K_a that has been observed experimentally. © *2008 American Institute of Physics*. [DOI: 10.1063/1.2992050]

I. INTRODUCTION

The three molecules HOOH, HSSH, and HSOH all have skew-chain equilibrium geometries. For each of them, the potential energy surface (PES) has two equivalent enantiomer minima described, for example, in Ref. 1. The energy splittings caused by tunneling between these minima (through torsion around an axis approximately coinciding with the bond between the two heavy nuclei) are sufficiently large for their effects to be observable in high resolution spectroscopic experiments. For the symmetrical molecules HOOH and HSSH, the energy level structure resulting from the torsional motion has been investigated in detail (see, for example, Refs. 2–8). The torsional splittings have been found to alternate with the parity of the rotational quantum number K_a. Hougen[9] (see also Hougen and DeKoven[10]) proposed a semiempirical model to explain this staggering of the splittings; in this model the 2π period of the torsional potential is extended to 4π (see below for the definition of the torsional angle). Alternating torsional splittings were also observed in the five-atomic skew-chain molecule HNCNH (Refs. 11 and 12) and explained in terms of the Hougen model.

High resolution rotational transitions of ground state HSOH, DSOD, and HSOD (Refs. 13–17) have been measured using the Cologne terahertz spectrometers.[17–19] Quite recently, the first high resolution measurements on HSOH in the midinfrared region have been performed using the Fourier transform spectrometer (IFS 120) at Wuppertal.[20,21] The experimental work has produced extremely accurate frequencies for observed assigned transitions involving states with $J \leq 40$ and $K_a \leq 4$. It is difficult to extend the measurements to higher K_a-values because high resolution spectrometers above 2 THz still pose a technical challenge. It was found that the experimentally derived torsional splittings do not stagger as in the cases of HOOH (Ref. 7) and HSSH (Refs. 4 and 5); they exhibit a more complicated variation with the rotational quantum number K_a. To explain the experimental findings, Yamada *et al.*[1] developed a semiempirical model for the rotation-torsion motion of HSOH analogous to the Hougen model for HOOH and HSSH.[9,10] The HSOH model involves an extension of the torsional-potential period to 6π and makes use of a symmetry group isomorphic to the C_{3v} point group described, for example, in Ref. 22. The theoretical results of Yamada *et al.*[1] lent credibility to the experimentally derived torsional-splitting pattern and thus to the assignment of the rotation-torsion spectrum of HSOH.[13,14,16] However, owing to the fact that HSOH has a lower symmetry than HOOH and HSSH, the semiempirical model for HSOH (Ref. 1) has more adjustable parameters than the analogous Hougen model for HOOH and HSSH.[9,10] In addition, the HSOH model has series expansions in the rotational quantum numbers J and K_a; these expansions are likely to

[a)]On leave from Institute of Applied Physics, Russian Academy of Science, Uljanov Street 46, Nizhnii Novgorod 603950, Russia.
[b)]On leave from Siberian Physical-Technical Institute, Tomsk State University, Novosobornaya Sq. 1, Tomsk 634050, Russia.
[c)]Author to whom correspondence should be addressed. Electronic mail: jensen@uni-wuppertal.de.

diverge at high rotational excitation. In consequence, as already noted in Ref. 1, the predictive power of the semiempirical model is limited.

Quack and Willeke[23] employed a quasiadiabatic channel quasiharmonic *reaction path Hamiltonian* (RPH) approach to study the vibrational energies of HSOH and its isotopomers $XSOY$ (X,Y=H, D, and T). Their calculations were based on an *ab initio* PES calculated at the MP2/aug-cc-pVTZ level of theory and produced a value of the $K_a=0$ torsional splitting for HSOH in very good agreement with the experimental value. However, no values of the splittings were computed for $K_a>0$, and so Ref. 23 has no bearing on the variation of the torsional splitting with K_a.

In the present work, we complement the work of Ref. 1 by taking a more direct approach to the calculation of the torsional splittings: We present variational calculations of the rotation-torsion energies of HSOH employing a newly computed *ab initio* PES for the ground electronic state. The surface was obtained at the CCSD(T) level of theory, using aug-cc-pV(Q+d)Z, aug-cc-pVQZ, and cc-pVQZ basis sets for S, O, and H, respectively.

The rotation-torsion energies of HSOH are calculated with the program TROVE (theoretical rovibrational energies)[24] using the geometries along the minimum energy path (MEP) of the torsional motion as the reference configuration. The other vibrations are viewed as displacements from the reference configuration. The idea of an adiabatic separation of large-amplitude and small-amplitude vibrations, the small-amplitude vibrations being defined as displacements from a flexible MEP reference configuration, was proposed in 1977 by Bunker and Landsberg,[25] whose ideas were based on the 1970 work by Hougen *et al.*[26] Bunker and Landsberg[25] applied the theory to a triatomic molecule, thus obtaining the *semirigid bender Hamiltonian*. Similar ideas were employed in 1980 by Miller *et al.*,[27] who formulated the RPH, which has been applied to HSOH by Quack and Willeke[23] and to a number of other molecules by other authors (see, for example, Refs. 28–31). We use here an implementation of the RPH approach where the "reaction coordinate" (or large-amplitude vibrational coordinate) is the torsional angle τ_{HSOH} (i.e., the dihedral angle between the plane containing the H–S–O moiety and that containing the S–O–H moiety). The Hamiltonian is expanded as a Taylor series in the coordinates describing the remaining small-amplitude vibrations (i.e., all vibrations other than the torsion), with the expansion being made around a geometry on the torsional MEP.

We aim at providing reliable predictions of the HSOH rotation-torsion energies, thus facilitating further analysis of the rotation-torsion spectra. We also aim at reproducing, in the *ab initio*-based calculations reported here, the observed variation with K_a of the HSOH torsional splittings and to provide further explanation of this variation.

The paper is structured as follows. In Sec. II we characterize the *ab initio* potential energy function used in the variational calculations. In Sec. III the variational method is described. The calculated rotation-torsional energies are compared to experiment in Sec. IV, where an empirical adjustment of the PES is also reported. We analyze our results in Sec. V and offer conclusions in Sec. VI.

II. THE *AB INITIO* POTENTIAL ENERGY SURFACE

We use here an *ab initio* potential surface for the electronic ground state of HSOH obtained by the CCSD(T) method (coupled cluster theory with all single and double substitutions from the Hartree–Fock reference determinant[32] augmented by a perturbative treatment of connected triple excitations[33,34]). The CCSD(T) energies were calculated with the MOLPRO2002 program package[35,36] in the frozen-core approximation. As mentioned above, we have used the aug-cc-pV(Q+d)Z basis set for S, the aug-cc-pVQZ basis set for O, and the cc-pVQZ basis set for H.[37–40] Further details of the *ab initio* calculations will be given elsewhere.[41] The *ab initio* PES obtained and the associated level of theory are referred to as AV(Q+d)Z.

The solution of the rotation-vibration Schrödinger equation is made in the framework of the RPH. The "reaction path" is taken as the MEP for the torsional motion, and the reaction coordinate is the torsional angle τ_{HSOH}. The MEP is determined by optimizing the structural parameters of HSOH (i.e., in an obvious notation, the three internuclear distances $r_{\mathrm{OS}}^{\mathrm{opt}}$, $r_{\mathrm{SH}}^{\mathrm{opt}}$, and $r_{\mathrm{OH}}^{\mathrm{opt}}$, together with the two bond angles $\alpha_{\mathrm{SOH}}^{\mathrm{opt}}$ and $\alpha_{\mathrm{OSH}}^{\mathrm{opt}}$) at 11 different values of τ_{HSOH} between 0° and 180°. The MEP obtained is shown in Fig. 1. Among the three internuclear distances, $r_{\mathrm{OS}}^{\mathrm{opt}}$ exhibits the strongest dependence on τ_{HSOH}, while $r_{\mathrm{OH}}^{\mathrm{opt}}$ varies very little. The bond angle $\alpha_{\mathrm{SOH}}^{\mathrm{opt}}$ varies more along the MEP than does $\alpha_{\mathrm{OSH}}^{\mathrm{opt}}$.

Along the MEP, the structural parameters $r_{\mathrm{OS}}^{\mathrm{opt}}(\tau)$, $r_{\mathrm{SH}}^{\mathrm{opt}}(\tau)$, $r_{\mathrm{OH}}^{\mathrm{opt}}(\tau)$, $\alpha_{\mathrm{SOH}}^{\mathrm{opt}}(\tau)$, and $\alpha_{\mathrm{OSH}}^{\mathrm{opt}}(\tau)$ (Fig. 1) depend on the torsional coordinate $\tau=\tau_{\mathrm{HSOH}}$, as indicated, and we model these functions as

$$a_X^{\mathrm{opt}}(\tau)=\sum_{k=0}^{4} a_k^X(\cos\,\tau-\cos\,\pi)^k, \tag{1}$$

where the optimized values of the expansion parameters a_k^X, where $k=0,\ldots,4$ and X=OS, SH, OH, SOH, or OSH, are listed in Table I. For each of the five functions $a_X^{\mathrm{opt}}(\tau)$, the five parameter values were obtained in a separate fitting to 11 input values; the root-mean-square (rms) deviations of these fittings are included in Table I.

In a TROVE calculation for a nonrigid molecule,[24] the "input" PES (denoted as type A in Ref. 42) is re-expanded around a flexible reference configuration, which, in the present case, is defined by the value of $\tau=\tau_{\mathrm{HSOH}}$ and of the bond lengths and angles $r_{\mathrm{OS}}^{\mathrm{opt}}(\tau)$, $r_{\mathrm{SH}}^{\mathrm{opt}}(\tau)$, $r_{\mathrm{OH}}^{\mathrm{opt}}(\tau)$, $\alpha_{\mathrm{SOH}}^{\mathrm{opt}}(\tau)$, and $\alpha_{\mathrm{OSH}}^{\mathrm{opt}}(\tau)$. The expansion is made in terms of internal linearized coordinates ξ_i^ℓ (Refs. 24 and 42), and for HSOH, these coordinates are given by

$$\xi_X^\ell=1-\exp(-a_X[r_X^\ell-r_X^{\mathrm{opt}}(\tau)]),\quad X=\mathrm{OS},\ \mathrm{SH},\ \mathrm{or}\ \mathrm{OH}, \tag{2}$$

where a_X is a molecular parameter for the stretching vibrations, and

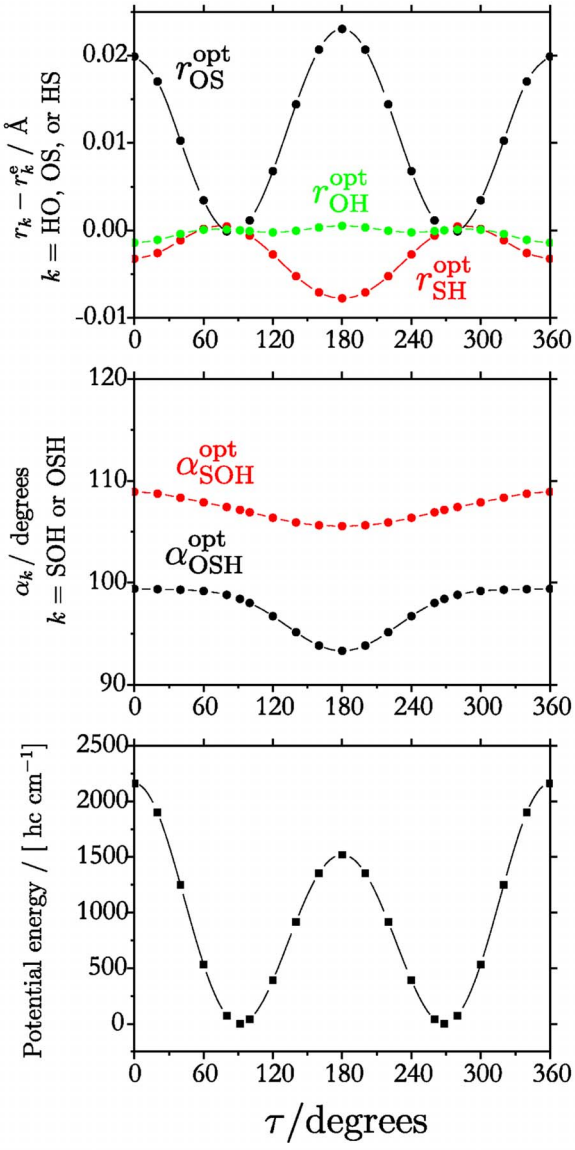

FIG. 1. (Color online) The variation of the optimized values of the bond lengths r_{OS}^{opt}, r_{SH}^{opt}, and r_{OH}^{opt} (top display), of the bond angles α_{OSH}^{opt} and α_{SOH}^{opt} (middle display), and of the *ab initio* energy (bottom display) along the MEP. All quantities are shown as functions of the torsional angle $\tau=\tau_{HSOH}$. For the bond lengths, we plot the deviations $r_{AB}^{opt}-r_{AB}^{(e)}$ from the equilibrium values $r_{OS}^{(e)}=1.667\ 25$ Å, $r_{SH}^{(e)}=1.34431$ Å, and $r_{OH}^{(e)}=0.96178$ Å (Ref. 41).

$$\xi_X^\ell = \alpha_X^\ell - \alpha_X^{opt}(\tau), \quad X = \text{OSH or SOH} \tag{3}$$

for the two bending vibrations. The coordinates r_X^ℓ and α_X^ℓ are linearized versions[22] of the geometrically defined coordinates r_X and α_X, respectively. The linearized coordinates are obtained by expanding the geometrically defined counterparts as first-order Taylor series in Cartesian displacement coordinates (see, for example, Sec. 10.4.2 of Ref. 22).

The re-expanded potential energy function is a type B PES, as defined in Ref. 42,

$$\begin{aligned} V(\xi_{OS}^\ell, \xi_{SH}^\ell, \xi_{OH}^\ell, \xi_{OSH}^\ell, \xi_{SOH}^\ell; \tau) &= V_0(\tau) + \sum_j F_j^\ell(\tau)\xi_j^\ell + \sum_{j,k} F_{jk}^\ell(\tau)\xi_j^\ell\xi_k^\ell \\ &+ \sum_{j,k,l} F_{jkl}^\ell(\tau)\xi_j^\ell\xi_k^\ell\xi_l^\ell + \sum_{j,k,l,m} F_{jklm}^\ell(\tau)\xi_j^\ell\xi_k^\ell\xi_l^\ell\xi_m^\ell, \end{aligned} \tag{4}$$

where the indices j, k, l, and m assume the values OS, SH, OH, OSH, and SOH. The expansion coefficients $V_0(\tau)$ and $F_{jk\ldots}^\ell(\tau)$ are given as tables of numerical values determined at a grid of equidistantly spaced τ-values τ_k and computed numerically with the central finite difference method employing quadruple (16 byte) precision.[24] As indicated in Eq. (4), in the present calculations the expansion of the type B PES is truncated after the fourth-order terms.

III. THE TROVE CALCULATIONS

The TROVE approach to the calculation of the rotation-vibration energies for molecules in isolated electronic states is described in Ref. 24, to which the reader is referred for details. Here we give a brief outline aimed at facilitating the understanding of the particular calculations done for HSOH.

When TROVE is adapted to do RPH calculations for HSOH, the molecular structures along the MEP define a flexible reference configuration, and the coordinates ξ_{OS}^ℓ, ξ_{SH}^ℓ, ξ_{OH}^ℓ, ξ_{OSH}^ℓ, and ξ_{SOH}^ℓ [Eqs. (2) and (3)], which describe the small-amplitude vibrations, measure displacements from this reference configuration. As already mentioned, the semirigid bender model by Bunker and Landsberg[25] is constructed according to this basic idea, and it implements the Sayvetz[43] condition in order to minimize the torsion-vibration interaction by eliminating certain terms in the rotation-vibration kinetic energy operator.[22] By contrast, the RPH approach of the present work minimizes the torsion-vibration interaction in the PES by letting the torsional MEP define the reference configuration.

In the current TROVE calculations, we use a kinetic energy operator expanded through second order in terms of the linearized coordinates ξ_i^ℓ, and so the total TROVE rotation-vibration Hamiltonian is given as an expansion similar to that in Eq. (4). Hence, it has a form well suited for an adiabatic separation of the small-amplitude vibrations from the

TABLE I. Expansion coefficients determining, through Eq. (1), the structural parameters along the torsional MEP in the electronic ground state of HSOH.

	a_0^X	a_1^X	a_2^X	a_3^X	a_4^X	$10^5\sigma$ [a]
r_{OS}^{opt} (Å)	1.690 363 0	−0.041 845 6	0.018 960 0	−0.001 253 5	0.000 914 1	5.0
r_{SH}^{opt} (Å)	1.336 516 0	0.011 876 5	−0.003 335 6	−0.000 594 5	−0.000 067 8	1.6
r_{OH}^{opt} (Å)	0.962 282 9	−0.003 101 2	0.003 894 1	−0.001 157 7	−0.000 125 7	1.0
α_{OSH}^{opt} (deg)	93.325 82	8.749 67	−4.242 54	0.610 91	0.041 55	3.2
α_{SOH}^{opt} (deg)	105.561 05	1.330 62	1.063 00	−1.102 00	0.328 23	2.4

[a]rms deviation of the fitting.

large-amplitude torsional motion. In the variational solution of the rotation-vibration Schrödinger problem, we numerically diagonalize a matrix representation of the rotation-vibration Hamiltonian, set up in terms of suitable basis functions. We make the adiabatic separation of the small-amplitude vibrations and the torsional motion because this leads to a very substantial reduction in the sizes of the matrix blocks to be diagonalized.

The basis functions used to construct the matrix representation of the rotation-vibration Hamiltonian are chosen as products of six functions, each of these functions being one dimensional (1D) in the sense that it describes one vibrational degree of freedom. That is, a basis function is given as

$$|\phi_{\rm vib}\rangle = |v_{\rm OS}\rangle|v_{\rm SH}\rangle|v_{\rm OH}\rangle|v_{\rm OSH}\rangle|v_{\rm SOH}\rangle|v_{\rm HSOH},\tau_{\rm tor}\rangle|J,K,\tau_{\rm rot}\rangle. \tag{5}$$

Each of the 1D small-amplitude vibrational basis functions $|v_X\rangle$ (where X=OS, SH, OH, OSH, and SOH, while v_X is the principal quantum number for the vibrational mode in question) depends on the coordinate ξ_X^ℓ and is determined in a solution of a reduced 1D Schrödinger equation by means of the Numerov–Cooley method.[44,45] The torsional basis functions $|v_{\rm HSOH},\tau_{\rm tor}\rangle$ [where $v_{\rm HSOH}$ is the principal torsional quantum number and $\tau_{\rm tor}$=0 or 1 determines the torsional parity[22] as $(-1)^{\tau_{\rm tor}}$] are determined by the Numerov–Cooley method[44,45] in the same manner as the $|v_X\rangle$ functions. The rotational basis functions $|J,K,\tau_{\rm rot}\rangle$ are symmetrized combinations of rigid-symmetric-top eigenfunctions,[22] where $\tau_{\rm rot}$ (=0 or 1) determines the rotational parity as $(-1)^{\tau_{\rm rot}}$ and the rotational quantum number $K=K_a$. For the RPH calculations of the present work, we use basis functions with $v_{\rm OS}=v_{\rm SH}=v_{\rm OH}=v_{\rm OSH}=v_{\rm SOH}=0$. That is, we expand the rotation-vibration eigenfunctions $\Psi_{J,\Gamma,i}$ as

$$\Psi_{J,\Gamma,i} = |0\rangle|0\rangle|0\rangle|0\rangle|0\rangle \times \sum_{v_{\rm HSOH},\tau_{\rm tor},K,\tau_{\rm rot}} C_{J,\Gamma,i}^{K,\tau_{\rm rot},v_{\rm HSOH},\tau_{\rm tor}} |v_{\rm HSOH},\tau_{\rm tor}\rangle \times |J,K,\tau_{\rm rot}\rangle, \tag{6}$$

where the $C_{J,\Gamma,i}^{K,\tau_{\rm rot},v_{\rm HSOH},\tau_{\rm tor}}$ are expansion coefficients and the $|0\rangle$ basis functions are associated with the redundant vibrational quantum numbers v_X=0, X=OS, SH, OH, OSH, and SOH. We have introduced Γ to denote the irreducible representation of the molecular symmetry group C_s(M) (see Table A-2 of Ref. 22) generated by the eigenfunction $\Psi_{J,\Gamma,i}$. The running index i labels eigenstates with the same values of J and Γ.

The energies computed by diagonalizing the matrix representation of the rotation-vibration Hamiltonian, set up in terms of basis functions as indicated in Eq. (6), can obviously be thought of as the eigenvalues of an effective rotation-torsion Hamiltonian obtained by averaging the complete rotation-vibration Hamiltonian over the small-amplitude vibrational motion. In practice, the use of only one basis function for each of the small-amplitude vibrational modes reduces very substantially the sizes of the matrices to be diagonalized, and so it becomes possible to employ very large torsional basis sets. This turned out to be essential for reaching a numerical accuracy sufficient to determine the very small torsional splittings, especially for high values of K. Calculations for $K\leq 5$ converge relatively fast as the basis set of Eq. (6) is increased, even at high J. However in order to achieve sufficient convergence for higher K, a very large torsional basis set was required: With $v_{\rm HSOH}\leq 41$, we could converge all rotational term values with $K\leq 12$ and the corresponding torsional splittings to within 0.0001 $\rm cm^{-1}$. As mentioned above, our basis functions are obtained by the Numerov–Cooley integration performed in quadruple-precision computations. In order to generate 84 torsional basis functions ($v_{\rm HSOH}\leq 41, \tau_{\rm tor}=0,1$), a very dense grid of 10 000 points was used. The use of a still denser grid was prohibited by the round-off errors associated with the Numerov–Cooley integration scheme even at 16 byte precision. This imposed a limit on the size of the torsional basis set at $v_{\rm HSOH}$=41. The convergence problem at higher K is apparently an indication of a deficiency of our torsional basis set at high rotational excitation. Probably, better convergence could be attained if the torsional basis functions were modified to depend on the quantum number K, as discussed in Ref. 42, and implemented, for example, for the bending vibration of triatomic molecules in Ref. 46.

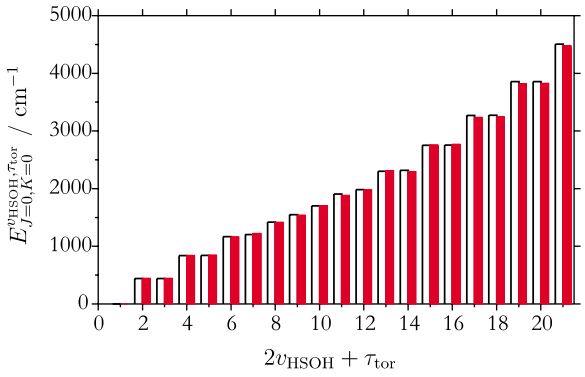

FIG. 2. (Color online) Comparison of torsional term values with $v_{\rm OS}=v_{\rm SH}=v_{\rm OS}=v_{\rm OSH}=v_{\rm SOH}=J=0$, computed using the RPH method (empty bars) with term values obtained in a full 6D variational calculation (filled bars) with the same PES (Ref. 41). The extended quantum number $2v_{\rm HSOH}+\tau_{\rm tor}$ gives the number of nodes for the wave function $|v_{\rm HSOH},\tau_{\rm tor}\rangle$.

With the TROVE program, it is straightforward to go beyond the adiabatic-separation approximation: All we need to do is to introduce small-amplitude vibrational basis functions [Eq. (5)] with $v_X>0$ (X=OS, SH, OH, OSH, and SOH). We have made such improved variational calculations to assess the accuracy of the RPH results. In Fig. 2 we compare the torsional term values (with $v_{\rm OS}=v_{\rm SH}=v_{\rm OH}=v_{\rm OSH}=v_{\rm SOH}=J=0$) computed using the RPH scheme to term values obtained in a full six-dimensional (6D) variational calculation with the same PES.[41] The "adiabatic" torsional term values closely follow the full-dimensional counterparts not only below 1000 $\rm cm^{-1}$, where the density of J=0 states is fairly low so that the states are not likely to experience resonances, but also in the energetically dense region above 1000 $\rm cm^{-1}$. For the details of the 6D variational calculation, see Ref. 41.

Another indication of the good performance of the model, important for the purposes of the present study, is that the RPH value for the J=0 torsional splitting in the vibrational ground state is obtained as 0.002 14 $\rm cm^{-1}$, in perfect

TABLE II. Rotation-torsion term values and torsional splittings for $J=4$ rotational levels in the vibrational ground state of HSOH, calculated with the TROVE program and compared to the corresponding experimental values.

Assignment				Term values $E(\mathrm{cm}^{-1})$					Splittings $\Delta_{\mathrm{tor}}(10^{-3}\ \mathrm{cm}^{-1})$				
J	K_a	K_c	τ_{tor}	Obs.	Calc.[a]	Δ[a,b]	Calc.[c]	Δ[b,c]	Obs.	Calc.[a]	Δ[a,d]	Calc.[c]	Δ[c,d]
4	0	4	0	10.046 956	10.001 781	0.045 175	10.050 369	−0.003 413					
4	0	4	1	10.049 109	10.003 805	0.045 304	10.052 519	−0.003 410	2.153	2.024	0.129	2.150	0.003
4	1	4	0	16.211 506	16.124 904	0.086 602	16.213 141	−0.001 635					
4	1	4	1	16.212 771	16.126 088	0.086 683	16.214 404	−0.001 633	1.265	1.184	0.081	1.263	0.002
4	1	3	0	16.358 850	16.271 590	0.087 260	16.361 102	−0.002 252					
4	1	3	1	16.360 110	16.272 770	0.087 340	16.362 361	−0.002 251	1.260	1.180	0.080	1.259	0.001
4	2	3	1	34.995 057	34.785 310	0.209 747	34.994 947	0.000 110					
4	2	3	0	34.996 830	34.787 054	0.209 776	34.996 790	0.000 040	1.773	1.744	0.029	1.843	−0.070
4	2	2	1	34.995 206	34.785 458	0.209 748	34.995 094	0.000 112					
4	2	2	0	34.996 980	34.787 202	0.209 778	34.996 937	0.000 043	1.774	1.744	0.030	1.843	−0.069
4	3	2	1	66.170 157	65.763 792	0.406 365	66.174 672	−0.004 515					
4	3	2	0	66.172 255	65.765 849	0.406 406	66.176 807	−0.004 552	2.098	2.057	0.041	2.135	−0.037
4	3	1	1	66.170 157	65.763 793	0.406 364	66.174 673	−0.004 516					
4	3	1	0	66.172 256	65.765 850	0.406 406	66.176 807	−0.004 551	2.099	2.057	0.042	2.134	−0.035
4	4	1	0	109.798 875	109.134 111	0.664 764	109.826 574	−0.027 699					
4	4	1	1	109.800 792	109.136 204	0.664 588	109.828 535	−0.027 743	1.917	2.093	−0.176	1.961	−0.044
4	4	0	0	109.798 875	109.134 111	0.664 764	109.826 574	−0.027 699					
4	4	0	1	109.800 792	109.136 204	0.664 588	109.828 535	−0.027 743	1.917	2.093	−0.176	1.961	−0.044

[a]Calculations with the AV(Q+d)Z *ab initio* PES.
[b]Obs−Calc. in units of cm^{-1}.
[c]Calculations with the refined PES (see text).
[d]Obs−Calc. in units of 10^{-3} cm^{-1}.

agreement with both the experimental value of 0.002 14 cm^{-1} (Ref. 1) and the value of 0.002 15 cm^{-1} from the 6D TROVE calculation. To obtain the theoretical splittings so accurately, however, a large torsional basis set with $v_{\mathrm{HSOH}} \leq 18$ had to be used.

IV. THE CALCULATED ROTATION-TORSION ENERGIES

In Table II, we list experimentally derived rotation-torsion term values $E(v_{\mathrm{HSOH}}, \tau_{\mathrm{tor}}, J, K_a, \tau_{\mathrm{rot}})$ for $J=4$ and compare them to the theoretical values obtained in the present work. (For brevity, we suppress in the table the redundant small-amplitude-vibrational quantum numbers $v_X=0$, where X=OS, SH, OH, OSH, and SOH.) The experimentally derived rotation-torsion term values and torsional splittings in Table II and, generally, in the remainder of the present paper are obtained from the HSOH spectra recorded in Cologne. Some of these experimental results have been published in Ref. 13. The complete list of term values for $J \leq 40$ is available as a supplementary material to this publication.[47] Table II also gives experimental and theoretical values for the torsional splittings $\Delta_{\mathrm{tor}}(v_{\mathrm{HSOH}}, J, K_a, \tau_{\mathrm{rot}}) = |E(v_{\mathrm{HSOH}}, \tau_{\mathrm{tor}}=1, J, K_a, \tau_{\mathrm{rot}}) - E(v_{\mathrm{HSOH}}, \tau_{\mathrm{tor}}=0, J, K_a, \tau_{\mathrm{rot}})|$. The table shows that for $J=4$, there is an excellent agreement between theory and experiment, and this level of agreement is typical for the entire data set available. The rms deviation for all experimentally derived torsional splittings (with $J \leq 40$ and $K_a \leq 4$) is 0.0002 cm^{-1}. The rotation-torsion term values are not reproduced quite so accurately by the AV(Q+d)Z *ab initio* PES. The corresponding rms deviation is 1.2 cm^{-1} for all experimentally derived term values (0.7 cm^{-1} for the term values with $J \leq 20$).

We have carried out an empirical adjustment of the PES in order to improve the agreement with experiment. In view of the fact that the rotational energies are strongly dependent on the molecular geometry through the moments of inertia, we decided to optimize the structural parameters a_0^X (X=OS, SH, OH), i.e., the constant terms in the expansions of Eq. (1). These parameter values determine the optimized structure of HSOH at the planar *trans* configuration with $\tau=180°$. The dependence of the energies on the angle parameters a_0^{OSH} and a_0^{SOH} turned out to be very slight so that these parameters need not be varied. The derivatives of the rotation-torsion term values with respect to the varied parameters a_0^X are required for the least-squares fitting. These derivatives were evaluated with the central finite difference method, and toward this end we computed for X=OS, SH, and OH the rotation-torsion term values for $a_0^X = a_0^{X,(0)} \pm \Delta a$, where $a_0^{X,(0)}$ is the *ab initio* parameter value and Δa is chosen as 0.01 Å. We carried out four iterations of the nonlinear least-squares fitting. In the first iteration, we fitted only term values with $J \leq 3$, but we extended the input data set to include all $J \leq 5$ term values in the second iteration, all $J \leq 10$ term values in the third iteration, and all $J \leq 20$ term values in the fourth iteration. In all four iterations, we used the derivatives calculated at the initial *ab initio* parameter values $a_0^{X,(0)}$. The refined values of the parameters are $a_0^{\mathrm{OS}} = 1.686\ 410$ Å, $a_0^{\mathrm{SH}} = 1.333\ 194$ Å, and $a_0^{\mathrm{OH}} = 0.957\ 740$ Å.

With the refined PES, we reproduce the experimental rotation-torsion term values with a rms deviation of 1.0 cm^{-1} (0.07 cm^{-1} for $J \leq 20$), and the experimentally derived torsional splittings (with $J \leq 40$ and $K_a \leq 4$) are reproduced with a rms deviation of 0.0002 cm^{-1} and a maximum deviation of 0.0012 cm^{-1}. The rms deviation has not de-

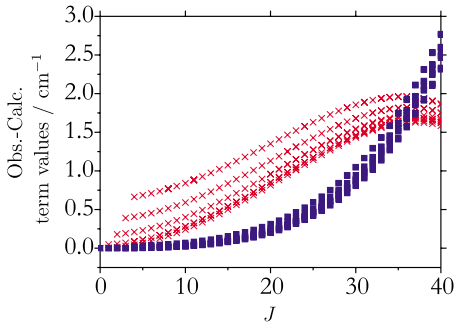

FIG. 3. (Color online) The residuals (Obs.−Calc.) for the rotation-torsion term values $E(v_{\mathrm{HSOH}}=0,\tau_{\mathrm{tor}},J,K_a,\tau_{\mathrm{rot}})$ of HSOH (in cm^{-1}). The residuals are calculated for all available experimentally derived term values (with $J\leq 40$ and $K_a\leq 4$) from the AV(Q+*d*)Z *ab initio* PES (red crosses) and the refined PES (blue squares), respectively. See text for further details.

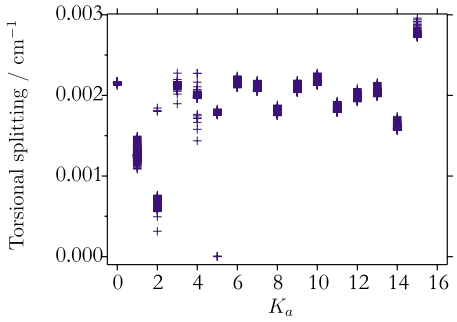

FIG. 4. (Color online) The theoretical values of the torsional splittings $\Delta_{\mathrm{tor}}(v_{\mathrm{HSOH}}=0,J,K_a,\tau_{\mathrm{rot}})$ (in cm^{-1}), plotted against the rotational quantum number K_a. For each K_a-value, we plot splittings calculated for $J=K_a,\ldots,40$ and $\tau_{\mathrm{rot}}=0$ and 1, with the refined PES. See text for further details.

creased relative to that obtained with the AV(Q+*d*)Z *ab initio* PES: The substantial improvement obtained for many splittings with low $J>0$ is canceled by a slight degradation for $J\geq 35$. The $J=4$ term values and torsional splittings computed with the refined PES are included in Table II. The effects of the empirical adjustment of the PES are illustrated in Fig. 3, where we show the residuals (Obs.−Calc.) of the rotational term values obtained with the AV(Q+*d*)Z *ab initio* PES and with the refined PES. For each PES, the term values with different K_a give rise to five parallel curves corresponding to $K_a=0,1,2,3,4$, respectively, with the $K_a=0$ term values producing the bottom curve and the $K_a=4$ term values producing the top curve. As mentioned above, as a result of the empirical adjustment, the agreement with experiment has improved substantially for term values with $J\leq 35$, while there is a slight degradation at the highest *J*-values considered. It is reassuring that the empirical adjustment has produced rather minor changes in the bond length parameters a_0^{OS}, a_0^{SH}, and a_0^{OH}. All three values have decreased in the fitting, but by less than 0.005 Å, which is probably within the error limits of the *ab initio* method employed. That is, the empirically adjusted parameters are very close to the *ab initio* values. This indicates that they are not unphysically effective values that merely reproduce well the input data used in the fitting. However we are cautious about claiming to have improved the HSOH geometry: At *J*-values above 40, our results start to diverge. This is probably caused by the fact that we truncate the expansion of the rotation-vibration Hamiltonian in the small-amplitude vibrational coordinates (Sec. III) after the second-order terms.

In Fig. 4 we plot the theoretically calculated torsional splittings $\Delta_{\mathrm{tor}}(v_{\mathrm{HSOH}},J,K_a,\tau_{\mathrm{rot}})$ against K_a. For each K_a-value, we plot splittings calculated for $J=K_a,\ldots,40$. The agreement with experiment for the splittings is illustrated in detail in Fig. 5, where we show the residuals (Obs.−Calc.) obtained for the available experimentally derived values. A comparison of Figs. 4 and 5 shows that the experimentally derived splittings are typically reproduced to a few percent. The agreement deteriorates slightly with increasing *J*, but the experimentally derived variation of the torsional splittings with K_a (Ref. 1) is obviously well reproduced by the calculations.

V. ANALYSIS

At present, for the HSOH molecule, experimentally derived torsional splittings have been determined for $K_a\leq 4$.[1,13,17] As mentioned above, the variation of the splittings with K_a for HSOH is very different from that exhibited by the symmetrical molecules HOOH and HSSH (see, for example, Refs. 2–8). For HSOH, Fig. 4 shows that, as discussed in Ref. 1, the torsional splittings vary somewhat erratically with K_a for the lowest K_a-values. For $K_a\geq 4$, the variation becomes more regular in that the splittings start to vary approximately periodically (with a period-of-three K_a-values) as K_a increases. Also for $K_a\leq 3$ the period-of-three pattern can be recognized for some values of *J*. This pattern is in accordance with the semiempirical model developed in Ref. 1. The periodicity derives from the fact that, as mentioned above, the rotational and torsional wave functions are usefully described in terms of a symmetry group called $C_{3v}^{(R)}$ in Ref. 1; this group is isomorphic to the C_{3v} point group.[22]

In Hougen's semiempirical model for the rotation-torsion motion in HOOH and HSSH,[9,10] the torsional motion can be completely separated from the rotation. That is, it is possible to consider one rotational state only, characterized by the quantum numbers *J*, K_a, and K_c (or, equivalently, by the quantum numbers *J*, K_a, and τ_{rot} as done in the present work), and to develop expressions for the torsional splittings in this particular rotational state. It is shown in Ref. 1 that no such complete separation is possible for the lower-symmetry

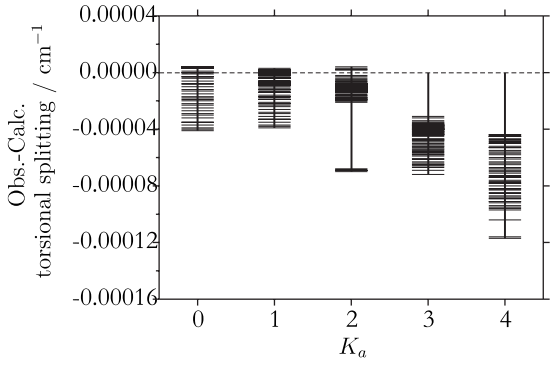

FIG. 5. The residuals (Obs−Calc.) obtained for the torsional splittings with the refined PES (see text).

TABLE III. Rotational term values E_{J,K_a}, torsional splittings Δ_{tor}, and asymmetry splittings Δ_{rot} (in cm^{-1}) for $J=10$ rotational levels in the vibrational ground state of HSOH, calculated with the TROVE program and the refined PES. See text for details.

K_a	E_{J,K_a}	Δ_{tor}	Δ_{rot} [a]
0	55.265 967	0.002 157	···
1	61.106 764	0.001 277	0.813686
2	80.222 288	0.000 668	0.013398
3	111.406 833	0.002 143	0.000052
4	155.057 849	0.001 969	···
5	211.181 217	0.001 763	···
6	279.776 960	0.002 100	···
7	360.844 521	0.002 051	···
8	454.383 926	0.001 750	···
9	560.395 572	0.002 037	···
10	678.879 055	0.002 125	···

[a]Only splittings $|\Delta_{\text{rot}}| \geq 10^{-6}$ cm^{-1} are given.

molecule HSOH. In the case of HSOH, it is necessary to consider together the two rotational states with common values of J and K_a but with $K_c=J-K_a$ or $J-K_a+1$, respectively (or equivalently with $\tau_{\text{rot}}=0$ or 1). The rotation-torsion energies for these two states are determined by diagonalization of a matrix involving the two rotational basis functions $|J,K_a,\tau_{\text{rot}}=0\rangle$ and $|J,K_a,\tau_{\text{rot}}=1\rangle$, both combined with torsional basis functions. Consequently, the torsional splittings depend not only on matrix elements associated with the terms in the Hamiltonian describing the torsion but also on the *asymmetry splitting* $\Delta_{\text{rot}}=|E_{\text{rot}}(J,K_a,J-K_a)-E_{\text{rot}}(J,K_a,J-K_a+1)|$, $K_a>0$, where $E_{\text{rot}}(J,K_a,K_c)$ is a rotational energy of HSOH, obtained in the approximation of neglecting the torsional motion. For example, for $K_a=3t\pm1$, where t is an integer, the torsional splittings are given by Eqs. (118) and (119) of Ref. 1, where Δ_{rot} is called $\Delta_{\text{rot}}^{(JK)}$.

It is well known (see, for example, Refs. 2, 3, and 48) that Δ_{rot} is largest for $K_a=1$ and decreases rapidly as K_a increases. In Table III we illustrate this by listing values of the rotational energies, torsional splittings, and asymmetry splittings obtained for HSOH at $J=10$. At $K_a=1$, $\Delta_{\text{rot}} \approx 0.8$ cm^{-1}, but already at $K_a=4$, $\Delta_{\text{rot}}<0.000\,000\,5$ cm^{-1}. We see that the onset of the regular period-of-three variation of the torsional splittings with K_a at $K_a=4$ (Fig. 4) coincides with Δ_{rot} becoming vanishingly small in comparison to Δ_{tor}. For $K_a \geq 4$, the torsional splittings are described in the "symmetric top limit" of Ref. 1, i.e., the limit of $\Delta_{\text{rot}} \to 0$ (see Fig. 9 of Ref. 1 and the discussion of it). For $K_a=1$ and 2, we have $\Delta_{\text{rot}} \gg \Delta_{\text{tor}}$, and so the torsional splittings are described by the limiting case discussed in connection with Fig. 7 of Ref. 1. According to Ref. 1, $K_a=3$ constitutes a special case with torsional splittings approximately equal to those for $K_a=0$, and this is borne out by the splittings plotted in Fig. 4.

In summary, by combining the theory of Ref. 1 with the results of the variational TROVE calculations from the present work, we can understand the variation of the torsional splittings with K_a: For $K_a=3t=0,3,6,9,\ldots$, the splittings are approximately equal, as explained in Sec. 5.2.1 of Ref. 1. The splittings for $K_a=1$ and 2 are described by the limiting case discussed in connection with Fig. 7 of Ref. 1 and vary somewhat irregularly, and the splittings for $K_a=3t\pm1\geq4$ are described in the symmetric top limit of Ref. 1 and vary regularly with a period of three K_a-values.

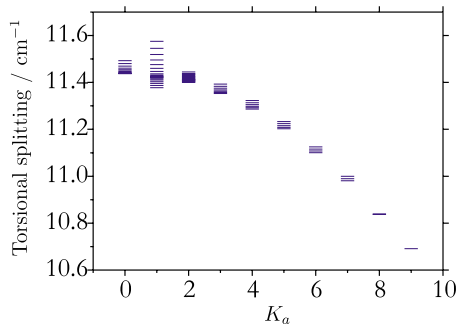

FIG. 6. (Color online) Torsional splittings in the vibronic ground state of HOOH.

In Fig. 6 we show the K_a-dependence of the torsional splittings in the vibrational ground state of HOOH, reconstructed from the experimental data as reported in Tables VI and VII of Ref. 7. Also here, there is some slight irregularity at $K_a=1$ and 2, which may be attributed to Δ_{rot} being much larger than Δ_{tor}, but the general trend is obviously different from that plotted for HSOH in Fig. 4. The staggering of the HOOH splittings (Sec. I) is not visible on the scale of Fig. 6.

As our calculations start to diverge for $K_a>12$ (which, as already mentioned, is probably caused by the fact that we truncate the expansion of the rotation-vibration Hamiltonian in the small-amplitude vibrational coordinates after the second-order terms), we cannot provide reliable predictions of the torsional splittings at these high K_a-values. One could surmise that the period-of-three variation continues to higher K_a and that eventually the splittings tend to zero.

To gain further insight into the mechanisms giving rise to the torsional splittings, we have analyzed a number of selected $J=10$ rotation-torsion eigenfunctions. In Fig. 7 we plot a reduced-density-of-states (RDoS) $\rho(v_{\text{HSOH}})$ diagram for states with $K_a=0$, 2, 4, 6, and 8. All these states are assigned to have $v_{\text{HSOH}}=0$, this assignment being obtained by the inspection of the pattern of rotation-torsion energies. The torsional RDoS $\rho(v_{\text{HSOH}})$ for a given state $\Psi_{J,\Gamma,i}$ [Eq. (6)] is defined as

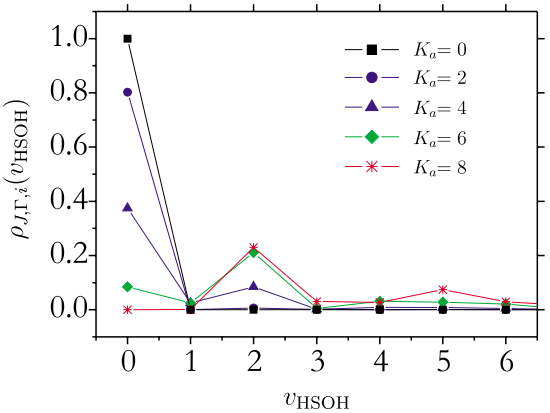

FIG. 7. (Color online) RDoS diagram [see Eq. (7) and the accompanying discussion] for rotational states of HSOH with $J=10$ and $K_a=0$, 2, 4, 6, and 8.

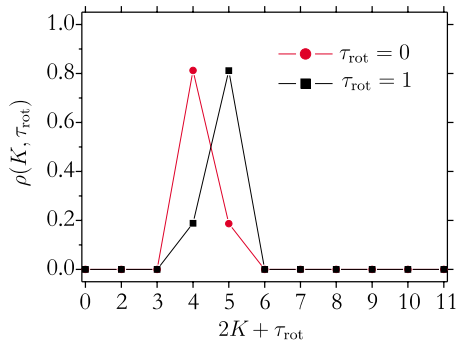

FIG. 8. (Color online) Rotational RDoS diagram [see Eq. (8) and the accompanying discussion] for rotational states of HSOH with $J=10$ and $K_a=2$.

$$\rho_{J,\Gamma,i}(v_{\mathrm{HSOH}}) = \sum_{K,\tau_{\mathrm{rot}},\tau_{\mathrm{tor}}} |C_{J,\Gamma,i}^{K,\tau_{\mathrm{rot}},v_{\mathrm{HSOH}},\tau_{\mathrm{tor}}}|^2. \quad (7)$$

According to Fig. 7, the state assigned to have $K_a=0$ has a 99.99% contribution from the basis function with $v_{\mathrm{HSOH}}=K=0$. The states assigned to have $K_a \geq 2$, however, are complex mixtures of torsional basis functions $|v_{\mathrm{HSOH}}, \tau_{\mathrm{tor}}\rangle$. Thus, for the two states assigned to have $K_a=2$ and 4, respectively, the contribution from the $v_{\mathrm{HSOH}}=0$ basis function is still largest, but the admixture from higher v_{HSOH}-values becomes significant. By contrast, the dominant contribution to the wave functions assigned to have $K_a=6$ and 8, respectively, originates in the $v_{\mathrm{HSOH}}=2$ basis function. At higher K, this effect is even more apparent. Thus the states at higher J suffer a strong centrifugal distortion mixing of different torsional basis functions. This, presumably, is another manifestation of the deficiency of our torsional basis set mentioned in Sec. III.

The rotational RDoS of states is given by

$$\rho_{J,\Gamma,i}(K, \tau_{\mathrm{rot}}) = \sum_{v_{\mathrm{HSOH}},\tau_{\mathrm{tor}}} |C_{J,\Gamma,i}^{K,\tau_{\mathrm{rot}},v_{\mathrm{HSOH}},\tau_{\mathrm{tor}}}|^2, \quad (8)$$

and we find that for each rotation-torsion state considered, a typical contribution around 99.99% arises from basis functions with one particular value of $K=K_a$ and $\tau_{\mathrm{rot}}=0$ or 1. Figure 8 is a rotational RDoS diagram for the states with $J=10$ and $K_a=2$. As explained in Ref. 1, there are four such states in total: Each of the two asymmetry-split rotational components (with $K_c=8$ and 9, respectively, for the states in Fig. 8) is further split into two torsional components. The wave functions corresponding to the two torsional components of a given rotational component have indistinguishable RDoS distributions. The RDoS distributions associated with the two rotational components are different, however, and are shown in Fig. 8. One of them has a dominant contribution of about 80% from the rotational basis function $|J=10, K=2, \tau_{\mathrm{rot}}=0\rangle$ (i.e., $2K+\tau_{\mathrm{rot}}=4$) and a remaining contribution of about 20% from the $|J=10, K=2, \tau_{\mathrm{rot}}=1\rangle$ ($2K+\tau_{\mathrm{rot}}=5$) basis function. We can obviously label this state as having $\tau_{\mathrm{rot}}=0$ from the dominant contribution to the wave function. For the other rotational component, the two significant contributions are simply interchanged, and we can label the corresponding state as having $\tau_{\mathrm{rot}}=1$. For each of the $K_a=2$ states in Fig. 8, we can identify a "dominant" τ_{rot}-value, but for higher K_a-values the wave functions become 50-50 mixtures of the $|J, K_a, \tau_{\mathrm{rot}}=0\rangle$ and $|J, K_a, \tau_{\mathrm{rot}}=1\rangle$ basis functions, and it eventually becomes impossible to make an assignment of the rotational component. Nevertheless, since the wave functions are given almost entirely in terms of the two rotational basis functions $|J, K_a, \tau_{\mathrm{rot}}=0\rangle$ and $|J, K_a, \tau_{\mathrm{rot}}=1\rangle$, K is a good quantum number in the calculations of the present work. This is the reason why the torsional splittings vary only weakly with J.

VI. SUMMARY AND CONCLUSION

We have generated a new *ab initio* CCSD(T)/aug-cc-pV(Q+*d*)Z PES (Ref. 41) for the electronic ground state of HSOH. Variational calculations of rotation-torsion energies have been performed with this surface in the framework of the RPH approach,[27] with the rotation-vibration Hamiltonian being expanded around geometries along the torsional MEP of HSOH. The calculated values of the torsional splittings are in excellent agreement with experiment; the rms deviation is 0.0002 cm^{-1} for all experimentally derived splittings (with $J \leq 40$ and $K_a \leq 4$). The available experimentally derived torsion-rotation term values (with $J \leq 40$ and $K_a \leq 4$) are reproduced *ab initio* with a rms deviation of 1.2 cm^{-1} (0.7 cm^{-1} for $J \leq 20$), which is improved to 1.0 cm^{-1} (0.07 cm^{-1} for $J \leq 20$) by empirically adjusting the three structural parameters $r_{\mathrm{SH}}^{\mathrm{opt}}$, $r_{\mathrm{OH}}^{\mathrm{opt}}$, and $r_{\mathrm{OS}}^{\mathrm{opt}}$ that characterize the optimized geometry at the planar *trans* configuration.

With the *ab initio* CCSD(T)/aug-cc-pV(Q+*d*)Z PES,[41] we calculate that the fundamental term value for the torsional mode is 451.7 cm^{-1}. The other fundamental term values are, in ascending order, 756.7 cm^{-1} (OS stretch), 1004.6 cm^{-1} (OSH bend), 1181.1 cm^{-1} (SOH bend), 2536.9 cm^{-1} (SH stretch), and 3657.2 cm^{-1} (OH stretch). The torsional fundamental term value is indeed the smallest one, but it amounts to 60% of the next one in the sequence associated with the OS stretching mode. Hence one may wonder whether it is appropriate to make an adiabatic separation of the torsional motion from the other vibrational modes such as we do here. However, we are chiefly interested in the torsional splittings, which are differences between close-lying energies, and it is to be expected that a substantial cancellation of errors takes place when the differences are formed. Also, the excellent agreement between theory and experiment, both for the term values and the splittings, lends credibility to our approach.

In consequence, we believe that our variational calculations provide reliable predictions for term values and splittings not yet observed. For example, in the spectra of HSOH,[17] which have recently been recorded with the Cologne sideband spectrometer,[19] some lines in the 1.9 THz region have been assigned to *c*-type transitions of the ${}^{r}R_4$-branch with lower-state J-values of 4, 5, and 6. Under the assumption that the splittings do not depend strongly on J, the observed line frequency splittings can be related to the tunneling splittings obtained for $K_a=4$ and 5, and with the known value of the $K_a=4$ splitting, a splitting of 48.5 MHz, corresponding to 0.001 62 cm^{-1}, is obtained at $K_a=5$. This

assignment is supported by the close agreement with the theoretical value of 0.001 763 cm^{-1} for this splitting (see Table III).

The calculated torsional splittings for HSOH are approximately equal for $K_a=3t=0,3,6,9,\ldots$. The splittings for $K_a=1$ and 2 vary somewhat irregularly, while those for $K_a=3t\pm1\geq4$ vary regularly and are repeated with a period-of-three K_a-values (Fig. 4). The theoretical values of the splittings are consistent with the experimental findings.[13,14,16] An analysis of the computational results in terms of a previously proposed semiempirical model[1] for the rotation-torsion motion has allowed us to explain the surprising variation of the torsional splittings with K_a.

We hope that the results of the present work will facilitate further experimental studies of HSOH.

ACKNOWLEDGMENTS

The authors thank Koichi M. T. Yamada for helpful advice. Part of this work was carried out while S.N.Y. and P.J. were visiting scientists, in the framework of the MEC research program FINURA (financed by the Spanish Government through Contract No. FPA2007–63074), at the Departamento de Física Aplicada, Facultad de Ciencias Experimentales of the Universidad de Huelva. They are extremely grateful, especially to Miguel Carvajal, for the kind hospitality extended to them and for financial support. They also acknowledge support from the European Commission through Contract No. MRTN-CT-2004–512202 "Quantitative Spectroscopy for Atmospheric and Astrophysical Research" (QUASAAR). The work of P.J. is supported in part by the Fonds der Chemischen Industrie, and that of S.N.Y. is supported by the Deutsche Forschungsgemeinschaft. R.I.O. is grateful for the partial support from the RFBR through Grant No. 06–02–16082-a.

[1] K. M. T. Yamada, G. Winnewisser, and P. Jensen, J. Mol. Struct. **695–696**, 323 (2004).
[2] G. Winnewisser, J. Chem. Phys. **56**, 2944 (1972).
[3] G. Winnewisser, J. Chem. Phys. **57**, 1803 (1972).
[4] S. Urban, E. Herbst, P. Mittler, G. Winnewisser, K. M. T. Yamada, and M. Winnewisser, J. Mol. Spectrosc. **137**, 327 (1989).
[5] P. Mittler, K. M. T. Yamada, and G. Winnewisser, Chem. Phys. Lett. **170**, 125 (1990).
[6] G. Winnewisser and K. M. T. Yamada, Vib. Spectrosc. **1**, 263 (1991).
[7] C. Camy-Peyret, J.-M. Flaud, J. W. C. Johns, and M. Noël, J. Mol. Spectrosc. **155**, 84 (1992).
[8] G. Pelz, K. M. T. Yamada, and G. Winnewisser, J. Mol. Spectrosc. **159**, 507 (1993).
[9] J. T. Hougen, Can. J. Phys. **62**, 1392 (1984).
[10] J. T. Hougen and B. DeKoven, J. Mol. Spectrosc. **98**, 375 (1983).
[11] M. Birk and M. Winnewisser, J. Mol. Spectrosc. **136**, 402 (1989).
[12] W. Jabs, M. Winnewisser, S. P. Belov, T. Klaus, and G. Winnewisser, Chem. Phys. **225**, 77 (1997).
[13] G. Winnewisser, F. Lewen, S. Thorwirth, M. Behnke, J. Hahn, J. Gauss, and E. Herbst, Chem.-Eur. J. **9**, 5501 (2003).
[14] M. Behnke, J. Suhr, S. Thorwirth, F. Lewen, H. Lichau, J. Hahn, J. Gauss, K. M. T. Yamada, and G. Winnewisser, J. Mol. Spectrosc. **221**, 121 (2003).
[15] S. Brünken, M. Behnke, S. Thorwirth, K. M. T. Yamada, T. F. Giesen, F. Lewen, J. Hahn, and G. Winnewisser, J. Mol. Struct. **742**, 237 (2005).
[16] O. Baum, S. Esser, N. Gierse, S. Brünken, F. Lewen, J. Hahn, J. Gauss, S. Schlemmer, and T. F. Giesen, J. Mol. Struct. **795**, 256 (2006).
[17] O. Baum, M. Koerber, O. Ricken, G. Winnewisser, S. N. Yurchenko, S. Schlemmer, K. M. T. Yamada, and T. F. Giesen, J. Chem. Phys. (submitted).
[18] G. Winnewisser, A. F. Krupnov, M. Y. Tretyakov, M. Liedtke, F. Lewen, A. H. Saleck, R. Schieder, A. P. Shkaev, and S. V. Volokhov, J. Mol. Spectrosc. **165**, 294 (1994).
[19] F. Lewen, E. Michael, R. Gendriesch, J. Stutzki, and G. Winnewisser, J. Mol. Spectrosc. **183**, 207 (1997).
[20] H. Beckers, S. Esser, T. Metzroth, M. Behnke, H. Willner, J. Gauss, and J. Hahn, Chem.-Eur. J. **12**, 832 (2006).
[21] O. Baum, T. F. Giesen, and S. Schlemmer, J. Mol. Spectrosc. **247**, 25 (2008).
[22] P. R. Bunker and P. Jensen, *Molecular Symmetry and Spectroscopy*, 2nd ed. (NRC Research, Ottawa, 1998).
[23] M. Quack and M. Willeke, Helv. Chim. Acta **86**, 1641 (2003).
[24] S. N. Yurchenko, W. Thiel, and P. Jensen, J. Mol. Spectrosc. **245**, 126 (2007).
[25] P. R. Bunker and B. M. Landsberg, J. Mol. Spectrosc. **67**, 374 (1977).
[26] J. T. Hougen, P. R. Bunker, and J. W. C. Johns, J. Mol. Spectrosc. **34**, 136 (1970).
[27] W. H. Miller, N. C. Handy, and J. A. Adams, J. Chem. Phys. **72**, 99 (1980).
[28] S. Blasco and D. Lauvergnat, Chem. Phys. Lett. **373**, 344 (2003).
[29] B. Fehrensen, D. Luckhaus, and M. Quack, Chem. Phys. Lett. **300**, 312 (1999).
[30] B. Kuhn, T. R. Rizzo, D. Luckhaus, M. Quack, and M. A. Suhm, J. Chem. Phys. **111**, 2565 (1999).
[31] B. Fehrensen, D. Luckhaus, M. Quack, M. Willeke, and T. R. Rizzo, J. Chem. Phys. **119**, 5534 (2003).
[32] G. D. Purvis and R. J. Bartlett, J. Chem. Phys. **76**, 1910 (1982).
[33] M. Urban, J. Noga, S. J. Cole, and R. J. Bartlett, J. Chem. Phys. **83**, 4041 (1985).
[34] K. Raghavachari, G. W. Trucks, J. A. Pople, and M. Head-Gordon, Chem. Phys. Lett. **157**, 479 (1989).
[35] MOLPRO, a package of *ab initio* programs written by H.-J. Werner and P. J. Knowles, Version 2002.3 and 2002.6, with contributions from R. D. Amos, A. Bernhardsson, A. Berning *et al.*
[36] C. Hampel, K. Peterson, and H.-J. Werner, Chem. Phys. Lett. **190**, 1 (1992), and references therein. The program to compute the perturbative triples corrections has been developed by M. J. O. Deegan and P. J. Knowles, *ibid.* **227**, 321 (1994).
[37] A. K. Wilson and T. H. Dunning, J. Chem. Phys. **119**, 11712 (2003).
[38] D. E. Woon and T. H. Dunning, J. Chem. Phys. **98**, 1358 (1993).
[39] R. A. Kendall, T. H. Dunning, and R. J. Harrison, J. Chem. Phys. **96**, 6796 (1992).
[40] T. H. Dunning, J. Chem. Phys. **90**, 1007 (1989).
[41] O. Baum, T. F. Giesen, S. N. Yurchenko, W. Thiel, V. V. Melnikov, R. I. Ovsyannikov, and P. Jensen (unpublished).
[42] S. N. Yurchenko, M. Carvajal, P. Jensen, H. Lin, J. J. Zheng, and W. Thiel, Mol. Phys. **103**, 359 (2005).
[43] A. Sayvetz, J. Chem. Phys. **7**, 383 (1939).
[44] B. Numerov, Mon. Not. R. Astron. Soc. **84**, 592 (1924).
[45] J. W. Cooley, Math. Comput. **15**, 363 (1961).
[46] P. Jensen, J. Mol. Spectrosc. **128**, 478 (1988).
[47] See EPAPS Document No. E-JCPSA6-129-021838 for a list of calculated HSOH rotation-torsion ($J\leq40$) term values. For more information on EPAPS, see http://www.aip.org/pubservs/epaps.html.
[48] D. Papoušek and M. R. Aliev, *Molecular Vibrational-Rotational Spectra* (Elsevier, Amsterdam, 1982).